EFFECTS OF SEA ICE RIDGES ON SOUND PROPAGATION IN THE ARCTIC OCEAN

by

O. I. Diachok
Naval Oceanographic Office

ABSTRACT

An environmental/acoustic model of sound propagation in the Arctic Ocean, which accounts for reflection losses from ridged sea ice, has been developed. In this model sea-ice ridges are represented as infinitely long, randomly distributed, elliptical half-cylinders. Under-ice reflection losses for acoustic wavelengths either large or small compared to ridge dimensions are computed from theoretical equations as a function of average keel depth and width, number of ridges per km, and grazing angle. Numerical values of under-ice reflection loss as a function of grazing angle are then incorporated into ray theoretical computations of transmission loss assuming a single sound speed profile which is characteristic of the central Arctic Ocean. The validity of the concepts, approximations, and the limitations of the model, and the accuracy of coincident measurements of environmental and acoustic parameters required to validate the model are discussed. To illustrate the predictions and accuracy of the model under diverse ice conditions, several comparisons of theoretical and experimental determinations of under-ice transmission loss in the central Arctic Ocean are presented.

INTRODUCTION

The environmental configuration of the Arctic Ocean is characterized by a relatively stable, nearly isothermal water column, and an ice canopy which is highly variable in both time and space.[1] Due to an essentially positive sound speed gradient in the water column, acoustic ray paths are generally upward-refracted and subsequently reflected and/or scattered from the ice-water interface[2] as illustrated in figure 1. Theoretically, reflection losses from the ice-water and ice-air interfaces are a function of frequency, and physical properties of the sea-ice canopy. A preliminary analysis[3] of coincident measurements of transmission loss and sea-ice ridge characteristics demonstrates that under-ice reflection loss at high frequencies may be quantitatively related to the average depth and number of ridges per km, suggesting that reflection loss at low frequencies may be similarly modeled.

The purpose of this paper is to (1) discuss geometrical and statistical models of sea ice ridges that lend themselves to quantitative analysis of under-ice reflection loss, (2) present a theoretical model of under-ice reflectivity which is consistent with the ridge models, (3) illustrate the effect of under-ice reflection losses on long range transmission loss and (4) compare theoretical predictions with experimental measurements of long range transmission loss, particularly at low frequencies.

Ideally, a demonstration of the validity of the model would require coincident measurements of long range transmission loss and under-ice ridge characteristics. Unfortunately, such measurements do not exist. Instead, a comparison will be made between transmission loss data and theoretical predictions based on estimates of ridge keel parameters, which were inferred from measurements of topside sea ice profiles and plausible models of sea-ice ridges.

Coincident measurements of topside sea-ice ridge characteristics and under-ice transmission loss, discussed in this paper, were acquired in May 1974 along tracks 18, 20, 22 and 26, which are depicted in figure 2.

MODELS OF SEA ICE RIDGES

Sea ice may be described as consisting of floating plates or floes about 3 m thick, occasionally interrupted by ridges, which are rubble piles formed by collisions and shear interactions between adjacent floes. Ridge dimensions vary widely but are nominally about 1 m high, 4 m deep and 12 m wide; the ridge length is generally much greater than the depth or width. A representative average spacing between ridges, which is random, is about 100 m. The effective orientation of a large number of ridges is also generally random. The cross-sectional contours of ridge sails and keels, the result of a random process, are highly variable.

A photograph depicting the two dimensional character of ridged sea ice,[4] as observed from aircraft, is illustrated in figure 3, as well as a coincident airborne laser profiler trace depicting the nature of the vertical profile of sea ice. Ridges are located at sites C, D and E.

Examples of measured cross-sectional ridge contours,[5,6,7] which are shown in figure 4, illustrate the following features of sea ice ridges: (1) a majority of ridge keels are flattened at the bottom due to ablation,[8] and approach the ice-water interface at a relatively steep angle, and (2) the shapes of ridge sails are highly variable, although in many instances a narrow protuberance is evident near the center of the ridge.

Measurements of the keel depth to sail height ratio, R, of previously reported contours[5,6,7,9] vary between 1/3 and 8, and average 4.0 ±0.5, as illustrated in the histogram[10] in figure 5. In this figure the number of observations is shown as a function of the estimated keel depth to sail height ratio of the examined contours. Another estimate of R, based on a statistical analysis[10] of a set of near-coincident measurements of about 100 keel depths and sail heights, results in R = 4.0 ±.3, which is in good agreement with the results in figure 5. In addition, it is noteworthy that the ratio between the deepest keel and the highest sail reported in the literature[6,10] is equal to 3.6.

A comparison between measured contours and simple geometrical shapes suggests that ridge keel contours may reasonably be represented by a half-ellipse, and that ridge sail contours may be described using the Gaussian distribution function,[10] as in figure 6. The relative dimensions of this geometrical model, in particular d/h = 4.0 and w_o/d = 1.6 are based on results shown in figure 5, previously reported measurements[10,20] of sea-ice ridge characteristics, and isostatic considerations.[1,10]

A theoretical investigation of acoustic reflectivity from a large number of sea-ice ridges also requires a model of the distribution of ridge heights, depths and widths. It has been suggested by Klimovich[12] and subsequently by the author[3] that the Rayleigh distribution function,[12] which is directly applicable to the description of the distribution of maxima of any random noise function, might also adequately describe the height/depth distributions of pressure ridges in sea ice. The distribution of widths has not been examined.

From a qualitative comparison between an empirical curve based on a large number of on-site measurements of ridge heights reported by Klimovich (corrected to height above the ice-water interface) and the Rayleigh distribution function shown in figure 7, it may be inferred that this function provides a reasonably good fit to Klimovich's representation of his set of measurements. Unfortunately, the corresponding raw data was not reported.

The systematic departure between the general trend of the measured data and Rayleigh distribution function in the region of small ridges may be a consequence of (1) measurement errors,[14] (2) the inadequacy of the Rayleigh distribution function to describe the observed distributions precisely, and (3) the nature of Klimovich's definition of a ridge, which unfortunately is not clearly stated.

Two statistical definitions[14,15,16,17] of a ridge have been proposed for computer analyses of airborne laser measurements of the distributions of ridge heights. A comparison between the distributions of ridge heights based on these definitions demonstrates that resultant distributions are virtually identical in the region of large ridges, but are strongly dependent on the statistical definition of a ridge in the vicinity of small ridges.[17,18]

Distributions of ridge heights derived from laser measurements, which are discussed in this paper, are based on the so-called Rayleigh criterion, viz. a relative maximum is a ridge when the corresponding minimum points are less than half of the peak. Based on this definition, the computed distribution of ridges approaches zero as the ridge height becomes large, and approaches infinity as the ridge height approaches zero, which is inconsistent with Klimovich's on-site observations in the region of small ridges, and with previously reported estimates[10] of the total number of

ridges per km. The unreasonably high counts in the region of small ridges are probably a result of considering snow drifts, floe edges and small "side-lobes" of large ridges as individual ridges. Consequently, only the distribution of relatively large ridges will be considered in comparisons with the theoretical function.

A comparison of the resultant distribution of ridge heights greater than 1.2 m, which was determined from laser measurements along two 300 km tracks in the western Arctic designated tracks 22 and 26, and the Rayleigh distribution function is shown in figure 8.

Due to the incomplete nature of the data, the theoretical curve had to be fitted to the data by selecting the total number of ridges, N and the characteristic ridge height, a ($a = 2/\sqrt{\pi}\, h$, where h is the average ridge height). In this case selection of N = 9.5 ridges per km, and a = 1.21 m provided the best fit to both sets of data, which are nearly identical.

For comparison, data based on laser measurements along two 300 km tracks in the eastern Arctic, designated tracks 18 and 20, is shown in figure 9. Here, selection of N = 11.5 ridges per km, and a = 1.48 m provided the best fit to the two data sets. These two sets of measurements are also virtually identical.

The inferred values of N are in quantitative agreement with Wittmann and Schule's results;[11] and the inferred values of h are in reasonably good agreement with Kovaks and Mellor[8] observations.

REFLECTION LOSS FROM RIDGED SEA ICE

Prior to a theoretical interpretation of the relationship between the statistical properties of sea-ice ridges and under-ice reflection loss, a few relevant theoretical aspects of acoustic reflectivity from sea ice will be mentioned.

Rays which propagate to long distances (greater than 30 km) in Arctic waters reflect from the ice-water interface at grazing angles, ϕ, which are generally smaller than 15°.

Representative values of the shear wave velocity[19] in bulk ice vary between 1500 and 1860 m/sec. If the lowest measured shear wave velocity is considered, the smallest possible shear critical (grazing) angle according to Snell's Law is 20°. Hence, if a simple ice-water interface is assumed, the theoretical reflectivity[20] at high frequencies in the angular range of interest is presumably unity over the reported range of sea ice velocities. Consequently, if the ice-water interface were perfectly smooth, the measured under-ice reflection loss might be expected to be zero. The sea ice canopy, however, is generally interspersed with ridges, and the estimated reflection loss is generally greater than zero.[3]

A theoretical model of reflectivity from a distribution of randomly spaced protuberances at a perfectly reflecting boundary has been developed by Twersky.[21,22] The model considers a plane acoustic wave incident on a one-dimensional distribution of protuberances, which may be either identical or non-identical, and either elliptic or circular half-cylinders situated at the surface of a perfectly reflecting half-space, as illustrated in figure 10.

The nature of "randomness" required is essentially that the average separation of the scatterers be large compared to widths, a condition that is generally satisfied by sea ice ridges. Based on the geometrical and statistical models discussed previously, the spacing-to-ridge-width ratio of sea ice ridges is estimated to be generally between 5 and 10, except in extremely rough near-shore areas during the winter season where this ratio may approach 2.

Approximate and relatively simple solutions for reflectivity have been derived by Burke and Twersky[22] as a function of grazing angle, ϕ, acoustic wave number, k, number of protuberances per unit distance, N, protuberance half-width, w, and depth, d, for cases where the wavelength is either large or small compared to protuberance dimensions. Theoretical solutions were derived for identical scatterers, but are equally valid for average values of d and w of non-identical scatterers.

To simplify the analysis of under-ice reflectivity in both the high and low frequency limits, the protuberance above the air-ice interface will be disregarded. Furthermore, at frequencies corresponding to wavelengths comparable to the modal thickness, complications caused by mode conversion to Lamb modes in the ice plate[23] will also be dismissed.

To apply results of Twersky's analysis to modeling under-ice reflection loss, the geometrical model in figure 10 will be assumed to be a good approximation of the spatial configuration of a large number of sea ice ridges. Due to the random orientation of ridges,[24] the effective ridge width, w, is assumed equal to $\sqrt{2}\, w_o$.

CASE 1: kd > 1

In this case the reflectivity from a distribution of widely spaced elliptical half-cylinders is independent of frequency; the wavelength is assumed to be smaller than the average ridge depth, d; and the plate thickness, a, is assumed to be infinitely large. The energy reflectivity, R, from a perfectly reflecting ridged surface is expressed by:

$$R = \left[\frac{1 - xnd/\phi}{1 + xnd/\phi}\right]^2 \qquad (1)$$

x may be interpreted as a correction for the eccentricity of the half-ellipse. For circular half-cylinders, x = 1; for the geometrical model of ridges under consideration, and in the angular range of interest, x = 0.9.

CASE 2: kd < 1

For the case where the wavelength is greater than the average ridge depth and the plate thickness, a, is assumed to be negligibly small, the energy reflectivity from a perfectly reflecting ridged surface is given by the expression:

$$R = 1 - 2\,(Nd)\,k^3 \left[d\left(\frac{d+w}{2}\right)^2 \right] \phi \qquad (2)$$

This equation is an approximate expression which is valid only for relatively small reflection losses.

Computed reflection losses as a function of grazing angle at frequencies of 30, 40 and 50 Hz and at high frequencies, shown in figure 11, are based on (a) estimates of N and h, inferred from laser measurements along tracks 22 and 26, (b) estimates of d and w inferred from the geometrical model, and (c) equations (1) and (2).

Computed reflection losses as a function of frequency and grazing angle, which are based on laser measurements along tracks 18 and 20, are delineated in figure 12.

From a comparison of the two sets of computations in figures 11 and 12, it may be inferred that losses at high frequencies are slightly higher in the eastern than western Arctic, whereas losses at low frequencies are much higher in the east than in the west. In accordance with this contention a

comparison[3] between previously reported transmission loss measurements[22,23,24] at various locations in the Arctic, and theoretical transmission loss computations which include a parametric surface reflection loss, also suggests that under-ice reflection losses are relatively high in the eastern Arctic.

COMPARISON BETWEEN THEORY AND EXPERIMENT

Theoretical computations of geometrical spreading loss are based on the sound speed structure along the measurement path, which is a function of temperature and salinity. Compared to ice-free oceans and seas, the temperature and salinity structure of the Arctic Ocean is relatively stable in time and uniform in space.[28] Quasi-synoptic measurements of vertical temperature profiles in the top 300 meters which were determined using bathythermographs at sites B, C, D, E, F and G, depicted in figure 3, are shown in figure 13. Also shown are temperature vs depth measurements made at T-3. These data illustrate the uniformity of the temperature structure in the top 300 meters and the slight variability of the structure in the top 50 meters. Below 300 meters the variability has been observed to be small.[28]

Measurements of vertical salinity profiles also reveal generally small differences, except in the Canadian Basin, where the near-surface salinity is demonstrably lower than in most other parts of the Arctic.[28] This anomaly, however, may be shown to have a small effect on sound speed.

The relative uniformity of temperature and salinity suggests that the velocity structure in the central Arctic Ocean may justifiably be approximated by a single vertical profile.

The effect of reflection loss on transmission loss may be computed using ray theory when the wavelength is small compared to environmental dimensions. Vibragrams depicting frequency vs. time of arrival of normal modes in the Arctic,[29] suggest that the departure from a ray theoretical description of sound propagation becomes pronounced at frequencies below about 40 Hz. Consequently, ray theoretical computations will be restricted to frequencies of 40 Hz and above.

Figure 14 indicates results of spatially averaged ray theoretical computations[30] of transmission loss based on a single sound velocity profile, which include surface reflection loss, as a function of grazing angle at frequencies of 40 Hz, 50 Hz and at high frequencies along the western Arctic tracks, designated 22 and 26. Ray theoretical computations represent the incoherent summation of 1000 rays between source angles of ±15°. A nominal angle-independent value of bottom loss of 1 dB per reflection was assumed in this set of computations. Effects of the ocean bottom on the magnitude of transmission loss for ranges greater than 30 km, however, are insignificant. At very low frequencies, where the wavelength becomes comparable to the ocean depth, bottom effects on the magnitude of transmission loss in Arctic waters may be considerable. Such low frequencies, however, will not be considered here.

Figure 14 also portrays coincident transmission loss measurements at frequencies of 40, 50 and 200 Hz, obtained by MK 61 explosive signals deployed from aircraft into water openings in the ice field, and detonated at a depth of 243 meters. The signals were detected at sites A and C (figure 2) at a depth of 90 meters via modified sonobuoys which were monitored from a second aircraft.

The data was tape-recorded and subsequently processed in one-third octave frequency bands and total energy transmission loss computed. Assumed values of source levels of explosive signals were based on results of Gaspin and Schuler.[31] (Data at 40 Hz were adjusted by 2 dB to facilitate demonstration of the virtual equivalence between predicted and measured loss per unit distance.)

Measurements and predictions of transmission loss along tracks 22 and 26 (figure 14) are in reasonably good agreement at both high (200 Hz), and low frequencies (40 and 50 Hz). Measurements at frequencies higher than 200 Hz are essentially identical to 200 Hz data up to a frequency of 800 Hz.

At higher frequencies other effects apparently become significant, as illustrated in figure 15(a). This figure shows the total attenuation coefficient above cylindrical spreading along tracks 22 and 26, previously reported absorption coefficients vs frequency corresponding to the North Pacific Ocean;[32,33] and a postulated curve depicting the absorption coefficient in the Canadian Basin which results in a "corrected" attenuation coefficient, which is independent of frequency as required by the under-ice reflection loss model. At 1 kHz a frequency-dependent attenuation coefficient, which is in excess of the frequency-independent attenuation due to under-ice reflection loss, is estimated to be .02 ±.01 dB/km.

This result is slightly lower than Mellen's[32] and Lovett's[33] estimate of the mid-water attenuation coefficient in the North Pacific Ocean, which at 1 kHz equals .035 ±.020 dB/km, and is significantly lower than attenuation measurements in the North Atlantic reported by Thorp,[34] which averages

.065 ±.020 dB/km at 1 kHz, as in figure 15(b). Simmons, et al.,[35] attribute the observed attenuation in this frequency range to a 1 kHz relaxation of boric acid, and suggest the possibility of a significant dependence on concentration. Consequently, it may be noteworthy that the near-surface salinity in the Canadian Basin, being between 27 and 31°/₀₀, is among the lowest in the world ocean.[28]

As previously reported, analysis of sound attenuation in the East Greenland Sea,[3] where the near-surface salinity is comparable to North Atlantic values, yields inferred mid-water attenuation coefficients in agreement with Thorp's results, as seen in figure 15(b).

Transmission loss was also measured along tracks 22 and 26 with explosive signals detonated at a depth of 18 m. A comparison between theoretical predictions and experimental measurements at a frequency of 200 Hz at the two source signal depths is illustrated in figure 16, as well as transmission loss computations corresponding to a surface reflection loss of zero. Agreement between theory and data for both source depths is excellent within a range of 150 km. This result is in accordance with previously reported measurements, which were generally limited to about 150 km. Beyond 150 km the general trend of the two sets of measurements departs from predicted curves. Discrepancies may be related to inaccuracies in the reflection loss model, and in ray theoretical computations. However, measurement errors caused by low signal to noise ratios, below 3 dB, at ranges beyond 150 km may also affect some of of the long range data.

Noticeably the prediction of the difference between the two sets of measurements at long ranges is reasonably accurate. At 200 km the predicted difference is 3 dB and the average measured difference is 5 dB.

Results of ray theory for transmission loss, including surface reflection loss at frequencies of 40, 50 and 200 Hz, corresponding to the eastern Arctic tracks, are shown in figure 17. Ocean depth along these tracks was about 1000 m.

Coincident transmission loss measurements at the same frequencies, also plotted in figure 17 were determined by explosives deployed from aircraft into water openings, and detonated at a depth of 243 m. In this case, however, the signals were detected at a depth of 60 m on hydrophones lowered from Ice Island, T-3, by H. Kutschale. (Data at 40 Hz were adjusted by 3 dB to facilitate demonstration of the virtual equivalence of predicted and measured loss per unit distance.) Again, predictions and measurements are in accord at both low and high frequencies.

DISCUSSION

The reasonably good agreement between theoretical predictions and experimental measurements along both eastern and western Arctic measurement tracks suggests that (1) the sea ice ridge model and theoretical distribution function, which were used to infer under-ice ridge characteristics from topside measurements are valid idealizations of ridged sea ice, (2) the assumption of horizontal uniformity of temperature and salinity in the Arctic Ocean is an acceptable approximation, and (3) predictions of the relatively simple reflection loss model are fairly accurate.

At high frequencies the dependence of reflection loss, R, on Nd, the product of the average ridge depth and number of ridges per km, is nearly linear for small Nd, whereas for large Nd the reflectivity asymptotically approaches zero. In the range of Nd considered in this paper the dependence of R on Nd is slight, and large uncertainties in Nd lead to small uncertainties in R. For example, $\Delta(Nd) = \pm 20\%$ results in $\Delta R = \pm 1$ dB in the range of angles where most of the energy which propagates to long ranges is concentrated.

Furthermore, uncertainties in the source levels of deep explosive signals at high frequencies are relatively well established,[30] and ray theory is expected to provide accurate estimates of transmission loss at high frequencies. As a consequence, agreement between predictions and measurements at high frequencies, particularly at ranges below 150 km, may be considered a demonstration of the validity of the reflection loss model.

Agreement at low frequencies, however, may to some extent be fortuitous. Owing to the dependence of theoretical reflection loss on the fourth power of ridge dimensions, the uncertainty in the experimentally determined average ridge depth and width must be below ±10% for the prediction of reflection loss to be meaningful. The procedure to estimate d and w, however, results in uncertainties in these parameters that have not been precisely ascertained. Furthermore, uncertainties in source levels at low frequencies, discussed in some detail by Weinstein,[36] may be greater than 3 dB. In addition, accurate computations of theoretical transmission loss at such low frequencies requires wave theory techniques.

CONCLUSIONS

Plausible geometrical and statistical models of sea-ice ridges have been described and a heuristic under-ice reflection loss model, based on these models has been developed.

The good agreement between theoretical computations of transmission loss including surface reflection loss and high frequency transmission loss measurements, reported previously as well as in this paper, may be considered demonstrations of the validity of the reflection loss model. At low frequencies the good agreement between predictions and measurements discussed in this paper suggests that the model is also valid at frequencies below 50 Hz. These results, however, may to some extent be fortuitous, and should not be considered reliable demonstrations of the validity of the model, due to uncertainties in the ridge model, reflection loss model, ray theory computations, and source levels.

A more convincing validation of the model at low frequencies would require a comparison between measurements of transmission loss from a source with a precisely known source level, and wave theoretical computations which include theoretical predictions of reflection loss based on coincident submarine sonar measurements of under-ice ridge characteristics. Unfortunately, such coincident measurements do not exist.

ACKNOWLEDGMENTS

This research was supported by the Naval Analysis Programs of the Office of Naval Research. The author is indebted to Gordon K. Long of the Acoustical Oceanography Division for performing the acoustic computations, Al Lohanick of the Polar Oceanography Division and Tim Daugherty of the

Physical Oceanography Division for processing the laser data, and Henry Kutschale of Lamont-Doherty Geophysical Observatory for collaborating on the acoustic measurements.

The author is grateful to Robert S. Winokur, Director, Acoustical Oceanography Division and Kenneth V. Mackenzie, Senior Staff Scientist of the Naval Oceanographic Office and Marvin Weinstein, Vice President of Underwater Systems, Inc., for reviewing the work, to Jane Mackenzie and my wife, Therese, for their editorial review, to Walter Wittmann, former Director of the Polar Oceanography Division, Naval Oceanographic Office, for his encouragement, and to Judy Albrittain for typing the manuscript.

The author is also indebted to the officers and crew of Oceanographic Development Squadron EIGHT, Patuxent Naval Air Station, Maryland, and to the participating scientists and technicians of the Naval Oceanographic Office, viz., Thomas Kozo, Jeffrey Kerling, Wayne Renshaw, Paul LaViolette, William Martin, James Parrott, Charles O'Neill and Frank Taylor, and in particular to Noel Belcher of the Fleet Weather Facility, for their dedication, cooperation and assistance throughout the course of the measurement program.

REFERENCES

1. N. M. Zubov, "L'dy Arktiki" (Arctic Ice), Chapter 7, Izdatel'stro Glavsevmorputi, Moscow. (1945)

2. A. R. Milne, "Sound Propagation and Ambient Noise Under Ice," Chapt. 7 in Underwater Acoustics, V. M. Albers, Ed., Phenum, Press, New York. (1967)

3. O. I. Diachok, "Effects of Sea Ice Ridge Characteristics on Under-Ice Reflection Loss in Arctic/Subarctic Waters," Proc. 8th Int. Cong. Acoustics, Symp. on Underwater Acoustics, Birmingham, England. (1974)

4. V. E. Noble, R. D. Ketchum and D. B. Ross, "Some Aspects of Remote Sensing as Applied to Oceanography," Proceedings of the IEEE, 57, 594-604. (1969)

5. T. L. Francois and W. E. Nodland, "Unmanned Arctic Research Submersible System Development and Test Report," University of Washington Technical Report No. APL-US 7219. (1972)

6. A. Kovaks, W. F. Weeks, S. Ackley and W. D. Hibler III, "Structure of a Multi-Year Pressure Ridge," Arctic, 26, 22-31. (1973)

7. W. F. Weeks and A. Kovaks, "On pressure ridges," Cold Regions Research and Engineering Laboratory Technical Report (unpublished). (1970)

8. A. Kovaks and M. Mellor, "Sea Ice Morphology and Ice as a Geologic Agent in the Southern Beaford Sea," in The Coast and Shelf of the Beaford Sea, J. C. Reed and J. E. Sater, Ed., Arctic Institute of North America, Arlington, Virginia. (1974)

9. T. L. Kan, S. C. Clay and J. M. Berkson, "Sonar Mapping of the Underside of Pack Ice," AIDJEX Bulletin, 21, 155-170. (1973)

10. O. I. Diachok, "A Simple Geometrical/Statistical Model of Sea Ice Ridges," submitted for publication to Geophysical Research Letters.

11. W. I. Wittmann and J. J. Schule, Jr., "Comments on the Mass Budget of Arctic Pack Ice," Proceedings of the Symposium on the Arctic Heat Budget and Atmospheric Circulations, the RAND Corporation Report No. 2M-5233-NSF. (1966)

12. V. M. Klimovich, "Characteristics of Hummocks in Shore Ice," Meteorology and Hydrology, 5, 84-93. (1972)

13. S. O. Rice, "The Mathematical Analysis of Random Noise," Bell Systems Tech. Journal, 23, 282-332. (1945)

14. R. T. Lowry, "An Experiment in Ice Profiling in Nares Strait and the Arctic Ocean," Proceedings of the Symposium on Remote Sensing in Glaciology, Cambridge, England, (in press).

15. E. Williams et. al., "A Submarine Sonar Study of Arctic Pack Ice," Proceedings of the Symposium on Remote Sensing in Glaciology, Cambridge, England (in press).

16. W. B. Tucker and V. S. Westhall, "Arctic Sea Ice Ridge Frequency Distributions Derived from Laser Profiler," AIDJEX Bulletin, 21, 171-180. (1973)

17. A. Lohanick, unpublished results.

18. W. D. Hibler, III, "Characteristics of Cold Regions Terrain Using Airborne Laser Profilometry." Proceedings of the Symposium on Remote Sensing in Glaciology, Cambridge, England, (in press).

19. K. Hunkins, "Seismic Studies of Sea Ice," J. Geophys. Res. 65, 3459-3476. (1960)

20. W. G. Mayer, M. Behravesh and T. Plona, "Sonic Reflectivity from Sea Ice/Water Interfaces," Georgetown University Technical Report. (1974)

21. V. Twersky, "On Scattering of Sound by Rough Surfaces," J. Acoust. Soc. Am., 29, 209-225. (1957)

22. J. E. Burke and V. Twersky, "On Scattering and Reflection by Elliptically Straited Surfaces," J. Acoust. Soc. Am. 40, 883-895. (1966)

23. O. I. Diachok and W. G. Mayer, "Ultrasonic Scattering from Polycrystalline Solids and Plates," J. Acoust. Soc. Am. 53, 946-947. (1973)

24. S. J. Mock et. al., "Spatial Aspects of Pressure Ridge Statistics," J. Geophys. Res., 77, p. 5945-5953. (1972)

25. B. M. Buck and C. R. Green, "Arctic Deep Water Propagation Measurements," J. Acoust. Soc. Am. 36, 1526-1533. (1964)

26. A. R. Milne, "A 90 km Sound Transmission Test in the Arctic," J. Acoust. Soc. Am. 35, 1459-1461. (1963)

27. H. Kutschale, previously unpublished measurements made during May 1968 and May 1970, under the sponsorship of the Office of Naval Research, Code 415.

28. L. K. Coachman and K. Aagard, "Physical Oceanography of Arctic and Subarctic Seas," in Marine Geology and Oceanography of the Arctic Seas, Y. Herman, Ed., Springer Virlag, New York. (1974)

29. H. Kutschale, "Arctic Hydroacoustics," Arctic, 22, p. 246-264. (1969)

30. B. G. Roberts, Jr., "Horizontal-Gradient Acoustical Ray Trace Program TRIMAIN," Naval Research Laboratory Technical Report. (1974)

31. J. B. Gaspin and V. K. Schuler, "Source Levels of Shallow Underwater Explosions," Naval Ordnance Laboratory Technical Report 71-160. (1971)

32. R. H. Mellen and D. G. Browning, "Low-Frequency Attenuation in the Pacific Ocean," (Abstract), 89th Meeting of the Acoustical Society, Austin, Texas. (1975)

33. J. R. Lovett, "Northeastern Pacific Sound Attenuation Using Low Frequency CW Sources," (unpublished).

34. W. H. Thorp, "Deep Ocean Sound Attenuation in the Sub- and Low-Kilocycle-per-Second Region," J. Acoust. Soc. Am. 38, 648-654. (1965)

35. V. P. Simmons, F. H. Fisher and S. A. Levinson, "Observation of the Low Frequency Relaxation in Sea Water Using a 200 Liter Glass Resonator," J. Acoust. Soc. Am. 56, II(A). (1974)

36. M. S. Weinstein and R. J. Hecht, "SUS Quality Assessment," Underwater Systems Inc. Technical Report (unpublished). (1973)

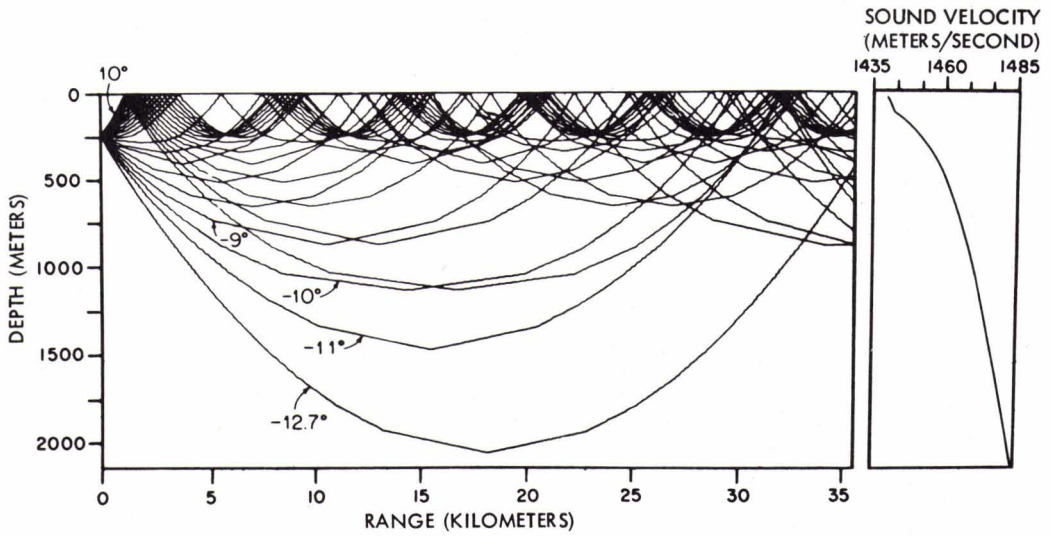

FIG. 1 TYPICAL SOUND SPEED PROFILE AND CORRESPONDING RAY DIAGRAM FOR SOUND PROPAGATION IN THE ARCTIC OCEAN

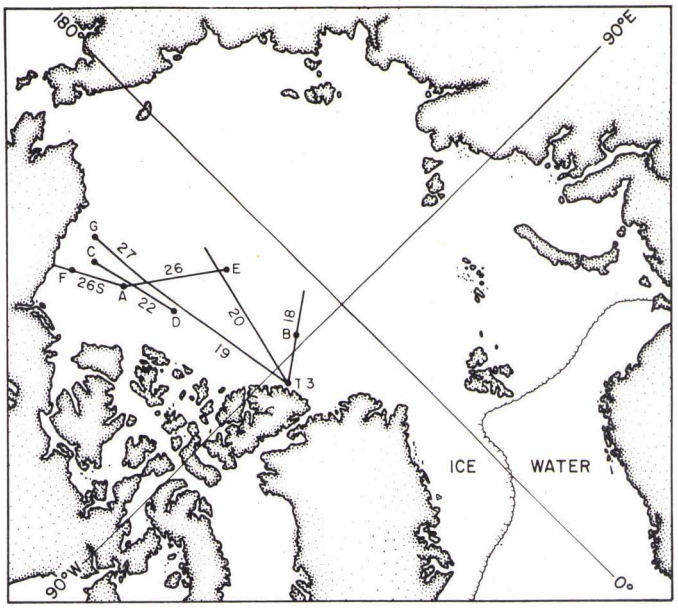

FIG. 2
LOCATIONS OF TRACKS, (18–26), ACOUSTIC MEASUREMENTS SITES (T–3, A, C and G), AXBT SITES (B–G) AND THE APPROXIMATE LOCATION OF THE ICE–WATER BOUNDARY

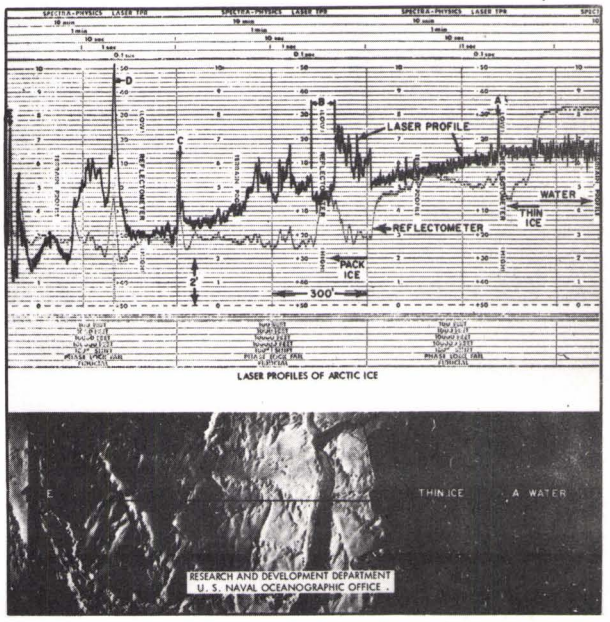

FIG. 3
COINCIDENT LASER MEASUREMENTS (top) AND PHOTOGRAPH (bottom) OF RIDGED SEA ICE NEAR ARCTIC ICE–WATER BOUNDARY. RIDGED ARE SHOWN AT SITES C, D AND E (Noble, Ketchum, and Ross)

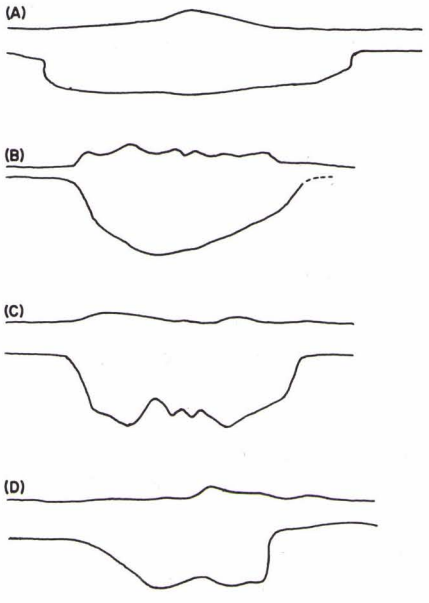

FIG. 4
RIDGE PROFILE MEASUREMENTS BY KOVAKS (A and B) AND FRANCOIS (C and D)

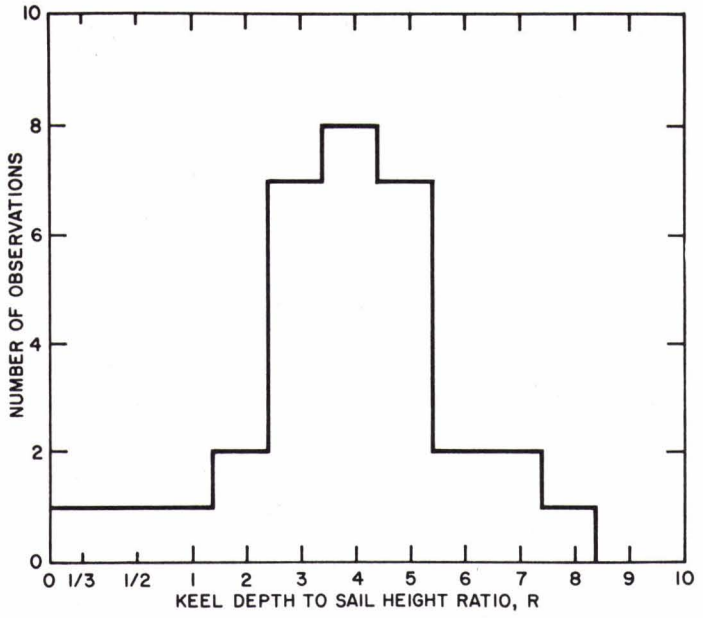

FIG. 5
HISTOGRAM OF THE NUMBER OF OBSERVATIONS vs ESTIMATED KEEL DEPTH TO SAIL HEIGHT RATIO

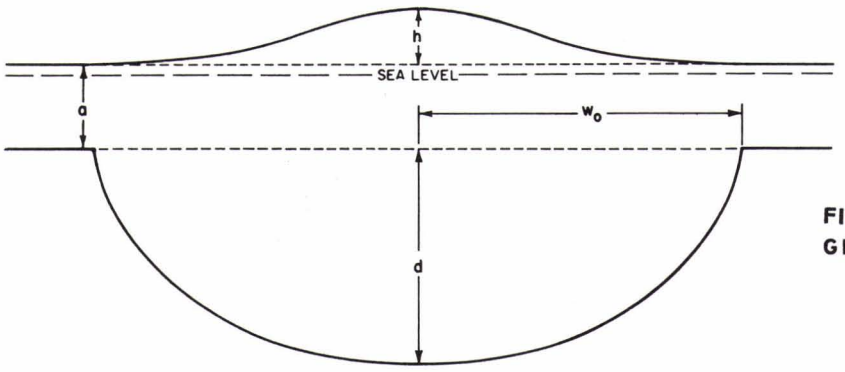

FIG. 6
GEOMETRICAL MODEL OF SEA-ICE RIDGES

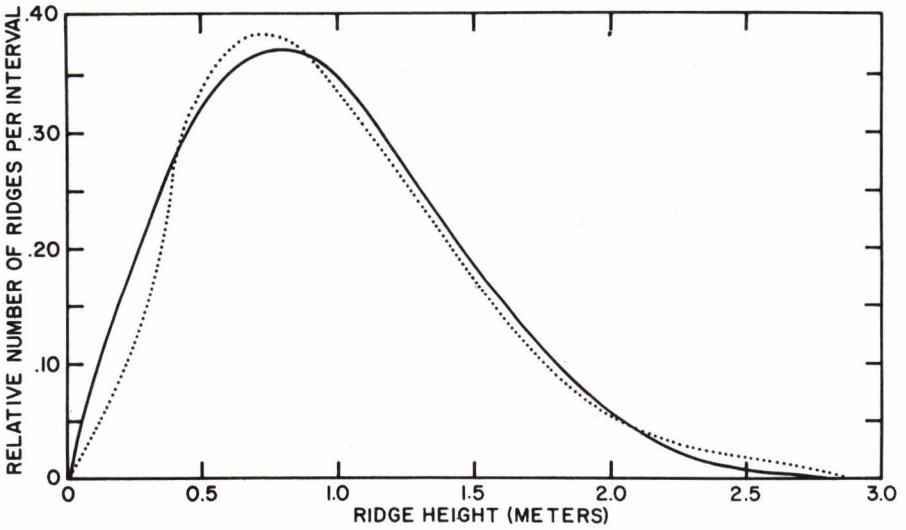

FIG. 7 COMPARISON BETWEEN KLIMOVICH'S EMPIRICAL CURVE (...) AND THE RAYLEIGH DISTRIBUTION FUNCTION (—)

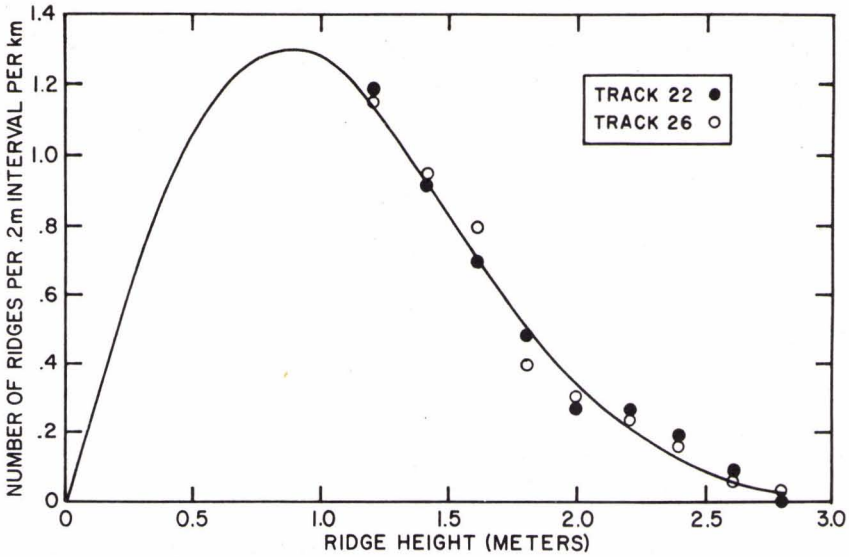

FIG. 8 NUMBER OF RIDGES PER 0.2 m INTERVAL PER km vs RIDGE HEIGHT ALONG TRACKS 22 AND 26, AND FITTED RAYLEIGH DISTRIBUTION FUNCTION. $N = 9.5\ km^{-1}$ AND $a = 1.21$ m

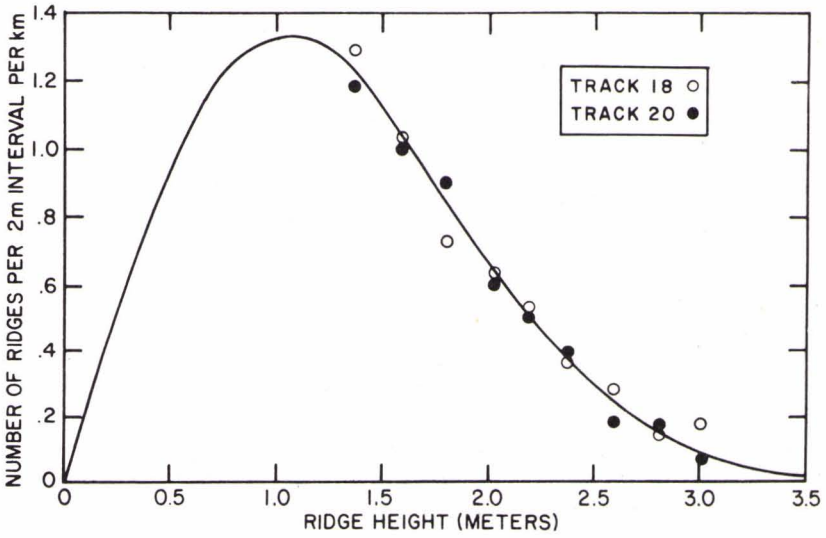

FIG. 9 NUMBER OF RIDGES PER 0.2 m INTERVAL PER km vs RIDGE HEIGHT ALONG TRACKS 18 AND 20, AND FITTED RAYLEIGH DISTRIBUTION FUNCTION. $N = 11.5\ km^{-1}$ AND $a = 1.48$ m

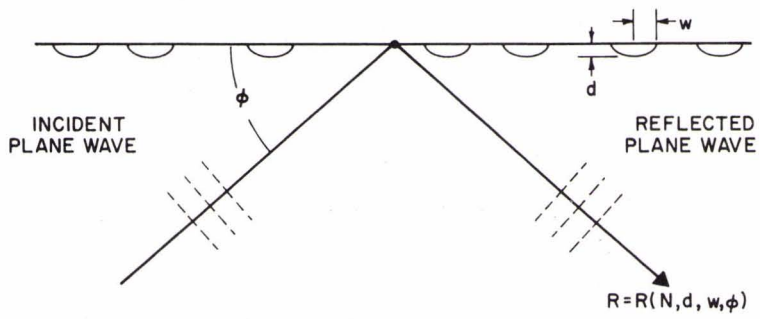

FIG. 10 GRAPHICAL REPRESENTATION OF PLANE WAVE SOUND REFLECTION FROM A RANDOM DISTRIBUTION OF ELLIPTICAL HALF-CYLINDERS

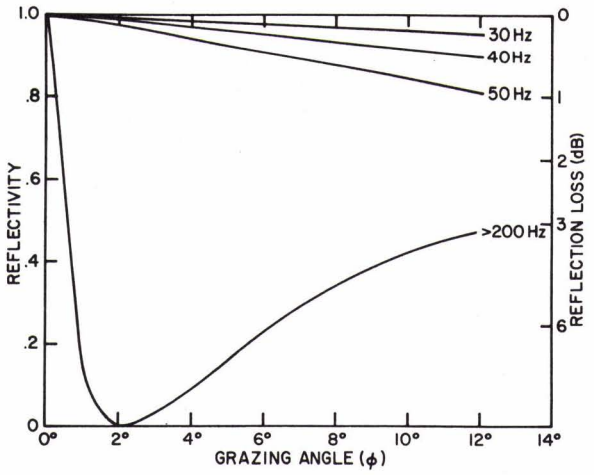

FIG. 11 COMPUTED REFLECTIVITY vs GRAZING ANGLE FOR FREQUENCIES OF 30, 40 AND 50 Hz AND HIGH FREQUENCIES. ESTIMATED RIDGE PARAMETERS : N = 9.5 km^{-1}, d = 4.3 meters, AND w = 9.8 m (TRACKS 22 AND 26)

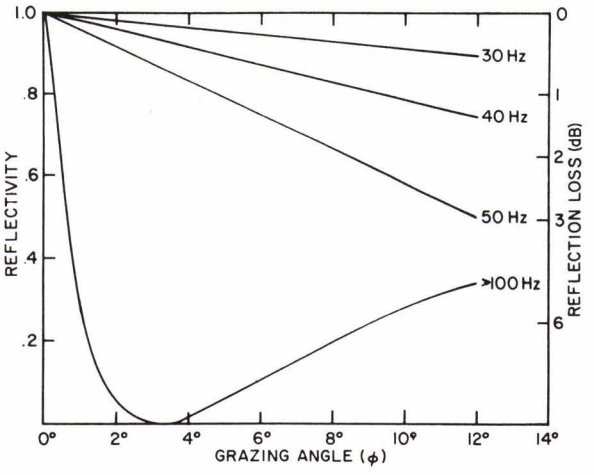

FIG. 12 COMPUTED REFLECTIVITY vs GRAZING ANGLE FOR FREQUENCIES OF 30, 40 AND 50 Hz AND HIGH FREQUENCIES. ESTIMATED RIDGE PARAMETERS : N = 11.5 km^{-1}, d = 5.3 meters, AND w = 11.9 m (TRACKS 18 AND 20)

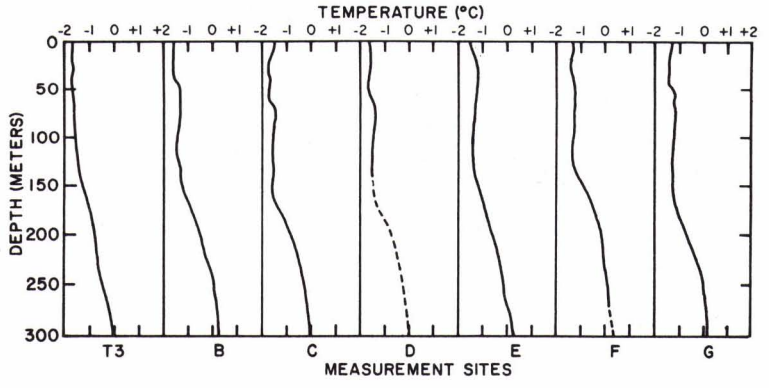

FIG. 13 AIRBORNE EXPENDABLE BATHYTHERMOGRAPHS RECORDED AT SITES B–G, AND TEMPERATURE vs DEPTH AT ICE ISLAND, T–3

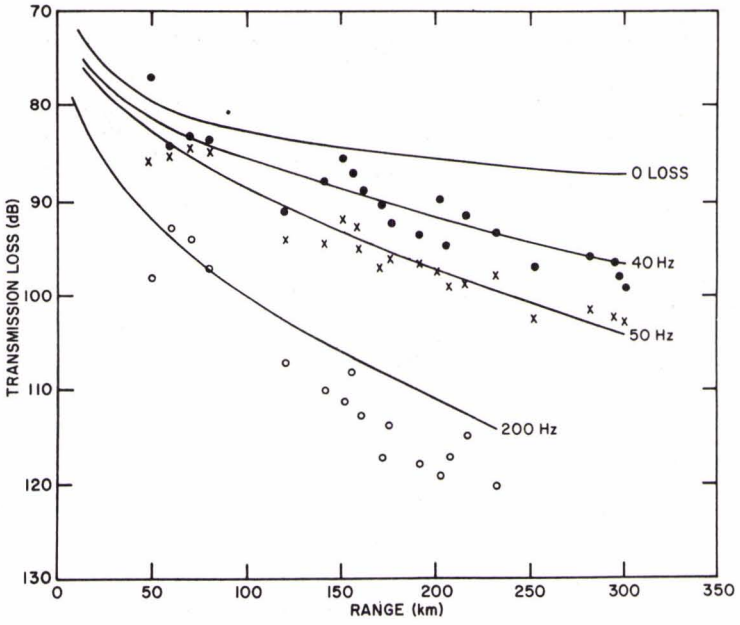

FIG. 14 COMPARISON OF THEORETICAL PREDICTIONS (—) AND EXPERIMENTAL MEASUREMENTS AT FREQUENCIES OF 40 Hz (•), 50 Hz (x) AND 200 Hz (o) ALONG TRACKS 22 AND 26

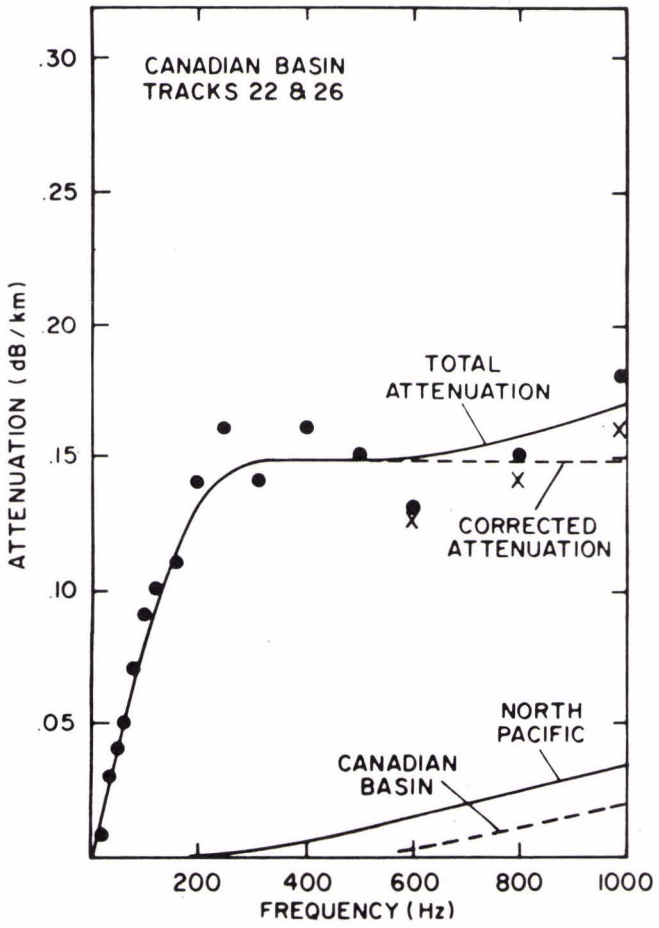

FIG. 15 (a)
TOTAL COMPUTED ATTENUATION (•) AND ATTENUATION CORRECTED FOR ABSORPTION (x), AND NORTH PACIFIC (—) AND ASSUMED CANADIAN BASIN (---) ABSORPTION COEFFICIENT vs FREQUENCY

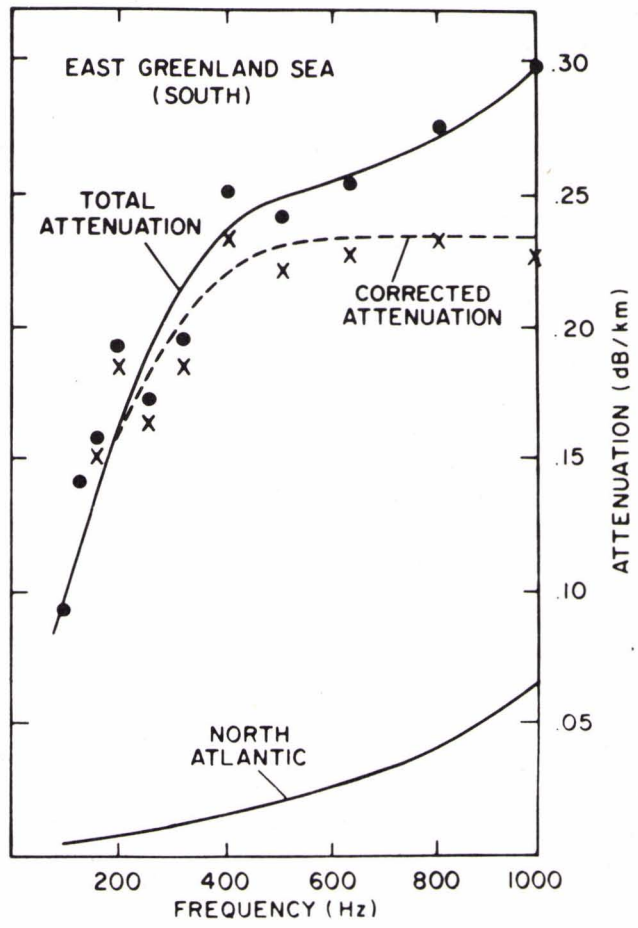

FIG. 15 (b)
TOTAL COMPUTED ATTENUATION (•) AND ATTENUATION CORRECTED FOR ABSORPTION (x), AND NORTH ATLANTIC (—) ABSORPTION COEFFICIENT vs FREQUENCY

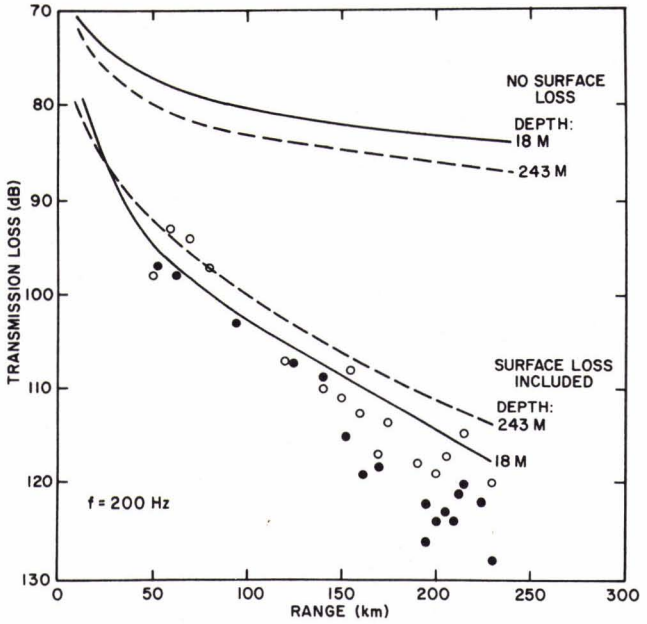

FIG. 16 COMPARISON BETWEEN PREDICTED (—) AND MEASURED (•) TRANSMISSION LOSS FOR SOURCE AT 18 m, AND PREDICTED (- - -) AND MEASURED (o) TRANSMISSION LOSS FOR SOURCE AT 243 m. RECEIVER AT 90 m. TRACKS 22 AND 26

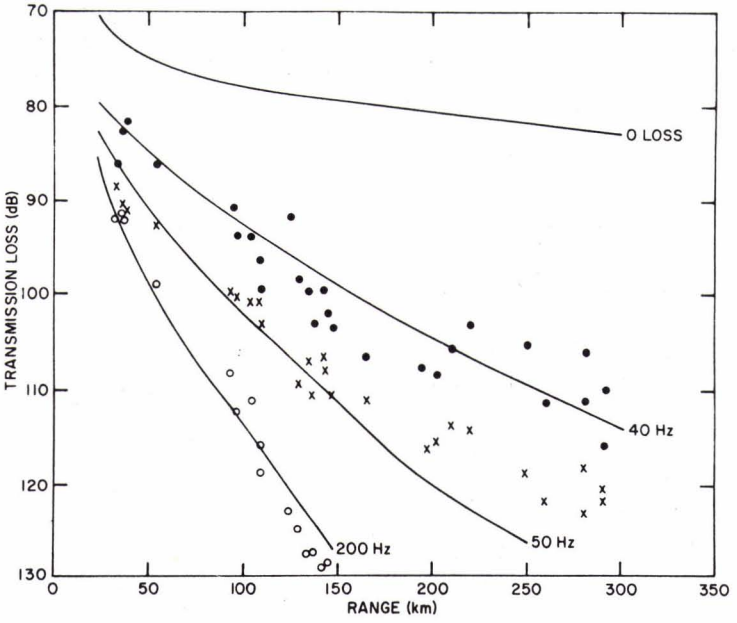

FIG. 17 COMPARISON OF THEORETICAL PREDICTIONS (—) AND EXPERIMENTAL MEASUREMENTS AT FREQUENCIES OF 40 Hz (•), 50 Hz (x) AND 200 Hz (o) ALONG TRACKS 18 AND 20